STIC-ILL

From: Lukton, David
Sent: Tuesday, April 20, 1999 5:32 PM
To: STIC-ILL

David Lukton
308-3213
AU 1654
SN 08/950542

* * * * * * * * * * * * *

AN 93372075 MEDLINE
DN 93372075

TI Separation of L-Pro-DL-boroPro into its component diastereomers and kinetic analysis of their inhibition of dipeptidyl peptidase IV. A new method for the analysis of slow, tight-binding inhibition.

AU Gutheil W G ; Bachovchin W W

SO BIOCHEMISTRY, (1993 Aug 31) 32 (34) 8723-31.
Journal code: A0G. ISSN: 0006-2960.

Biochemistry

 Volume 32, Number 34 August 31, 1993

Articles

Separation of L-Pro-DL-boroPro into Its Component Diastereomers and Kinetic Analysis of Their Inhibition of Dipeptidyl Peptidase IV. A New Method for the Analysis of Slow, Tight-Binding Inhibition†

William G. Gutheil and William W. Bachovchin*

Department of Biochemistry, Tufts University School of Medicine, Boston, Massachusetts 02111

Received November 30, 1992, Revised Manuscript Received May 12, 1993

ABSTRACT: The potent dipeptidyl peptidase IV (DP IV) inhibitor [1-(2-pyrrolidinylcarbonyl)-2-pyrrolidinyl]boronic acid (L-Pro-DL-boroPro) [Flentke, G. R., Munoz, E., Huber, B. T., Plaut, A. G., Kettner, C. A., & Bachovchin, W. W. (1991) *Proc. Natl. Acad. Sci. U.S.A. 88*, 1556-1559] was fractionated into its component L-L and L-D diastereomers by C18 HPLC, and the binding of the purified diastereomers to DP IV was analyzed. Inhibition kinetics confirms that the L-L diastereomer is a potent inhibitor of DP IV, having a K_i of 16 pM. The L-D isomer binds at least 1000-fold more weakly than the L-L, if it binds at all, as the ~200-fold weaker inhibition observed for the purified L-D isomer is shown here to be due entirely to the presence of a small amount (0.59%) of the L-L diastereomer contaminating the L-D preparation. The instability of Pro-boroPro, together with its very high affinity for DP IV and the time dependence of the inhibition, makes a rigorous kinetic analysis of its binding to DP IV difficult. Here we have developed a method which takes advantage of the slow rate at which the inhibitor dissociates from the enzyme. The method involves preincubating the enzyme and the inhibitor without substrate and then assaying the free enzyme by the addition of substrate and following its hydrolysis for a period of time which is short relative to the dissociation rate of the inhibitor. Data from experiments in which the preincubation time was sufficient for enzyme and inhibitor to reach equilibrium were analyzed by fitting to an appropriate form of the quadratic equation and yielded a K_i value of 16 pM. Data from experiments in which the incubation time was insufficient to establish equilibrium, *i.e.*, within the slow-binding regime, were analyzed by fitting to an integrated rate equation. The appropriate integrated rate equation for an $A + B \rightleftharpoons C$ system going to equilibrium does not appear to have been previously derived. The analysis of the slow-binding curves yielded a K_i value of 16 pM, in agreement with that of 16 pM determined in the equilibrium titrations, and a bimolecular rate constant of association, k_{on}, of 5.0×10^6 M^{-1} s^{-1}. The experimentally determined k_{on} and K_i indicate that the dissociation rate constant, k_{off}, is 78×10^{-6} s^{-1} ($t_{1/2}$ = 150 min). The slow-binding curves are shown here to fit a simple $E + I \rightleftharpoons EI$ model, indicating that it is not necessary to invoke a two-step mechanism to explain the inhibition kinetics.

Dipeptidyl peptidase IV (DP IV) is a type II membrane-anchored serine exoprotease found on the proximal tubules of the kidney (Gossrau, 1985; Wolf *et al.*, 1978), in the intestinal [illegible] the surface of certain subsets of T lymphocytes, particularly CD4+ helper cells (Ansorge & Ekkehard, 1987; Scholz *et al.*, 1985; Mentlein *et al.*, 1984), and in a number of other tissues

0006-2960/93/0432-8742$04.00/0

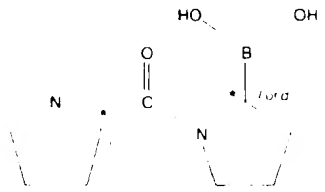

trans Pro-boroPro

FIGURE 1: Structure of *trans*-Pro-boroPro showing chiral centers. The coupling of L-Pro with racemic D-boroPro is expected to yield a mixture of two diastereomers. L-Pro-L-boroPro and L-Pro-D-boroPro.

(Schön *et al.*, 1985; Flentke *et al.*, 1991). Specific inhibitors of DP IV are therefore of some interest, both as tools to help elucidate the biological role or roles of DP IV and as potential therapeutic agents.

We have previously reported the synthesis and a preliminary kinetic characterization of two potent inhibitors of DP IV, Ala-boroPro and Pro-boroPro (boroPro refers to an analog of proline in which the carboxylate group is replaced by a boronyl group) (Bachovchin *et al.*, 1990; Flentke *et al.*, 1991). These inhibitors have an immunosuppressant activity, suppressing antigen-induced T-cell proliferation in T-cell culture systems (Flentke *et al.*, 1991) and antibody production in mice (Kubota *et al.*, 1992). These findings lend support to the hypothesis that DP IV plays a role in T-cell proliferation and suggest that DP IV inhibitors may be of therapeutic value.

Ala-boroPro and Pro-boroPro belong to a class of serine protease inhibitors known as peptide boronic acids (Kettner & Shenvi, 1984). Inhibitors of this class can have remarkably high affinities for their target enzymes. For example, MeO-Suc-Ala-Ala-Pro-boroPhe inhibits chymotrypsin with a K_i of 160 pM (Kettner & Shenvi, 1984), and Ac-D-Phe-Pro-boroArg inhibits thrombin with a K_i of 41 pM (Kettner *et al.*, 1990). The potency of these inhibitors is widely attributed to the ability of the boronyl group to form a tetrahedral adduct with the active site serine, which closely mimics the transition state of the enzyme-catalyzed reaction (Koehler & Lienhard, 1971; Lindquist & Terry, 1974; Rawn & Lienhard, 1974; Philipp & Maripuri, 1981; Bachovchin *et al.*, 1988). The peptide moiety, however, must also contribute importantly to the affinity, as simple alkyl- and arylboronic acids are many orders of magnitude less effective as inhibitors. X-ray crystallography and NMR spectroscopy have confirmed the presence of a boron–serine tetrahedral adduct in several serine protease peptide boronic acid inhibitor complexes. However, NMR spectroscopy has also demonstrated that in certain cases tetrahedral boron histidine adducts are formed (Bachovchin *et al.*, 1988; Tsilikounas *et al.*, 1992).

The more potent peptide boronic acid inhibitors usually inhibit their target enzymes in a time-dependent manner (Kettner & Shenvi, 1984; Shenvi, 1986; Kettner *et al.*, 1988, 1990), a phenomenon known as slow-binding inhibition [reviewed in Morrison and Walsh (1988)]. Both Ala-boroPro and Pro-boroPro are slow-binding inhibitors of DP IV. Morrison and Walsh (1988) have postulated that most, if not all, slow-binding inhibitors bind to their target enzymes in two steps, *i.e.*, the inhibitor first forms a relatively weak

proteases is not yet clear, but is of considerable theoretical interest as it should have important implications, both for understanding the catalytic mechanism of serine proteases and for the rational design of inhibitors.

A major impediment to the study of slow-binding inhibition is that the kinetic analysis is not trivial. The high affinity these inhibitors typically have for their target enzymes means that kinetic experiments must often be carried out under conditions where $I \approx E$ and, thus, where the approximation that $I_{free} = I_{total}$, which greatly simplifies the kinetic analysis of weaker binding inhibitors, is no longer valid. The time dependence of the inhibition further complicates matters because it may prevent a steady-state rate from being reached until substrate depletion becomes significant. Such a system is described by a set of differential equations for which an integrated rate equation is not available, although expressions have been derived for the case where substrate depletion is not significant during the time course of inhibitor binding (Cha, 1975, 1976).

The kinetic analysis of Ala-boroPro and Pro-boroPro binding to DP IV is even more complicated because these inhibitors are unstable, having half-lives of about 5 and 30 min, respectively, at neutral pH. In the preliminary kinetic analysis we reported K_i values of 2 and 3 nM, respectively, for Ala-boroPro and Pro-boroPro, realizing that these values substantially overestimated the true K_i values owing to the simplified way in which K_i determinations were carried out and to the instability and slow binding of these inhibitors (Flentke *et al.*, 1991). The original analyses were also carried out with inhibitors which were diastereomeric mixtures, *i.e.*, L-Ala-DL-boroPro and L-Pro-DL-boroPro. The expectation is that only one of the isomers, presumably the L-L isomer, is the active inhibitor.

Because the potency of these inhibitors is unusually high for such small molecules, and because DP IV appears to have important biological functions, a more detailed analysis of how these small dipeptide boronic acids interact with DP IV should be of considerable interest. Here we report (i) the purification of L-Pro-L-boroPro and L-Pro-D-boroPro from the L-DL diastereomeric mixture and (ii) a more detailed kinetic analysis of each isomer's inhibition of DP IV. To circumvent the difficulties outlined above, we have developed a method which exploits the fact that dissociation of the inhibitor from the enzyme is a relatively slow process. The method involves incubating the enzyme with inhibitor in the absence of substrate. The amount of free enzyme at any time can then be determined by adding substrate and monitoring the time course of the enzyme-catalyzed reaction for a short period during which the inhibitor does not have time to measurably dissociate from the enzyme. These simplified experimental conditions allow the derivation of expressions which can be used to analyze inhibitor binding under both equilibrium and nonequilibrium conditions. Equilibrium conditions here refer to experiments in which the preincubation time was sufficient for enzyme and inhibitor to reach equilibrium prior to the addition of substrate and enzyme assay. Nonequilibrium conditions refer to experiments in which the preincubation time was insufficient for equilibrium to be reached, and thus the system is within the slow-binding time domain. The integrated rate equation needed to analyze the nonequilibrium data does not appear to have been previously derived and is therefore derived here for the first time. This approach and the derived equations should prove useful in the analysis of

MATERIALS AND METHODS

Preparation of L-Pro-L-boroPro and L-Pro-D-boroPro Diastereomers by HPLC. Pro-boroPro was synthesized as described

previously (Bachovchin *et al.*, 1990). Analytical and semi-preparative C18 HPLC were performed on a 250 × 4.6 mm 5-μm Nucleosil C18 HPLC column (Alltech Associates Inc., Deerfield, IL) using a Hewlett-Packard 1050 quaternary pump HPLC equipped with a multiple wavelength detector (Hewlett-Packard, Rockville, MD). Several milligrams of the purified components could be prepared by repeatedly injecting 0.5 mg of the mixture on this column and then pooling and lyophilizing the appropriate fractions. The resulting material was redissolved in 0.01 N HCl. Analytical C18 HPLC chromatograms of the purified products are shown in Figure 2. The absolute configurations were assigned on the basis of a detailed NMR study (J. L. Sudmeier, W. G. Gutheil, and W. W. Bachovchin, unpublished results). An attempt to scale up this purification procedure on 200 × 10 mm and 400 × 10 mm Absorbosphere C18 HPLC columns (Alltech Associates) did not provide as pure a final product.

Quantitation of Pro-boroPro by Amino Acid Analysis. Amino acid analysis was performed by the PITC method (Bidlingmeyer *et al.*, 1984). Quantitation was based on proline. The boronylproline did not appear in this analysis.

Purification of Pig Kidney DP IV. Pig kidney DP IV was prepared as described previously (Wolf *et al.*, 1978). The concentration of DP IV active sites was assessed by stoichiometric titration with L-Pro-L-boroPro, as described further below.

Standard DP IV Enzyme Assays. Standard activity assays were performed in 50 mM sodium phosphate (pH 7.5) at 25 °C with the chromogenic substrate Ala-Pro-*p*-nitroanilide (APPNA) (Bachem Inc., Torrance, CA), monitoring the A_{410} on a Hewlett-Packard UV–vis spectrometer. The value $\Delta\epsilon$ = 8800 M^{-1} cm^{-1} upon hydrolysis of substrate was used to calculate rates and concentrations (Erlanger *et al.*, 1961). The hydrolysis time course was monitored for 2 min. The initial substrate concentration was 73.7 μM, 5 times the K_m (*vide infra*).

Equilibrium Titrations of DP IV with L-L *and* L-D *Pro-boroPro.* These experiments were performed by first preparing a DP IV stock in the assay buffer. The amount of DP IV used in each assay was the minimal amount necessary to obtain a sufficient absorbance change in 2 min with the substrate for accurate quantitation. A series of Pro-boroPro dilutions and a blank were prepared in 0.01 N HCl. To 0.980 mL of the stock-diluted DP IV was added 10 μL of diluted Pro-boroPro, the mixture was incubated for 30 min at 25 °C, and the free enzyme was assayed by the addition of APPNA in 10 μL of DMF.

Kinetics of DP IV and L-*Pro*-L-*boroPro Association.* For the association kinetics a fluorometric assay with Ala-Pro-7-amino-4-(trifluoromethyl)coumarin (APAFC) (Enzyme Systems Products, Livermore, CA) was used. Fluorescence was monitored on a Perkin-Elmer LS-5 fluorescence spectrometer (Oak Brook, IL) with an excitation wavelength of 400 nm and a detection wavelength of 505 nm. The response was calibrated with 1 μM 7-amino-4-(trifluoromethyl)-coumarin. The experiments were performed by incubating DP IV with inhibitor in the absence of substrate. After an appropriate time interval, APAFC was added to assay for free DP IV. The slow apparent rate of DP IV–inhibitor association under these dilute conditions gave a time course [illegible] (Figure 5). Specifically, experiments were performed [illegible] stock DP IV in assay buffer [illegible] concentration [illegible] used in the equilibrium binding experiments. A blank assay on the diluted DP IV was performed by mixing 0.990 mL of the diluted enzyme with 10 μL of 1 mM APAFC in DMF in a cuvette (10 μM final concentration) and monitoring the fluorescence change for 2 min at 25 °C. This value was considered to be t = 0 for the binding time course. An aliquot of L-Pro-L-boroPro was then added to the remaining 9.010 mL of diluted DP IV, and 0.990-mL aliquots were removed and assayed at intervals with APAFC as above.

Stability of L-L *and* L-D *Pro-boroPro.* In 0.01 N HCl these compounds appeared stable for at least 1 month at room temperature. Both the L-L and L-D Pro-boroPro preparations lose their DP IV inhibitory activity in the assay buffer at pH 7.5. To partially characterize this behavior, the time course of inactivation was monitored at three different concentrations: two at relatively low inhibitor concentrations, using DP IV inhibition as an indicator of residual inhibitor concentration, and one at relatively high inhibitor concentration, using C18 HPLC to determine residual inhibitor concentration. For inactivation in the range of inhibitor used in the assays above, the inhibitor was diluted into assay buffer at a concentration sufficient to give roughly 90% inhibition initially (approximately 1 nM for the L-L and 100 nM for the L-D). At various time intervals DP IV was added, and after a 15-min incubation, APPNA was added to assay for the free enzyme analogous to the procedure used in the equilibrium titrations. In a second experiment the inhibitor concentration in the pH 7.5 buffer was 100 times the assay concentration. At time intervals between 1 and 150 min, 10 μL of the Pro-boroPro solution was added to 0.980 μL of assay buffer containing DP IV, and this mixture was allowed to incubate for 15 min. Substrate was then added to assay for free enzyme. The inhibition observed in these experiments was converted to the amount of active inhibitor using the inverse to the equilibrium relationships as derived in the Theory section. The inactivation of these compounds was also observed directly at higher concentrations (250 μM) by analytical C18 HPLC. Half-lives ($t_{1/2}$) for degradation were determined empirically from plotted degradation time courses as the time at which one-half of the inhibitor remained.

Progress Curves for Enzyme + Substrate + Inhibitor Assays. These experiments were performed in two ways. One was for the enzyme to be added to an assay mixture containing a known amount of both the substrate and the inhibitor. The other was to incubate the enzyme with inhibitor for 15 min to establish equilibrium and then add substrate. The control for this experiment was to monitor a complete time course for the hydrolysis of substrate by enzyme.

Numerical Inetegration of Rate Equations. Numerical integrations of rate equations were performed with the GEAR software package (Stabler & Chesick, 1978; McKinney & Weigert, 1986).

Data Analysis. Data were analyzed by fitting to the appropriate equation by derivative-free nonlinear regression using the IBM PC based version of the BMDP program AR (BMDP Statistical Software, Los Angeles, CA). The equations used are derived in the Theory section.

THEORY

Derivation of Equations Describing Simple $A + B \rightleftharpoons C$ Equilibrium. In the enzymatically monitored equilibrium titrations, we are titrating DP IV with Pro-boroPro. The concentration of the stock Pro-boroPro is accurately known [illegible] Pro-boroPro was serially diluted, and this principle allows the concentration of DP IV to be accurately determined by titration. A simple $A + B \rightleftharpoons C$ equilibrium can be solved

exactly using the quadratic equation. Using E_T to represent the total DP IV concentration and I_T to represent the total inhibitor concentration, the following equations can be derived:

$$(EI) = \frac{(E_T + I_T + K_i) - \sqrt{((E_T + I_T + K_i)^2 - 4E_TI_T)}}{2} \quad (1)$$

$$E = E_T - (EI) \quad (2)$$

$$I = I_T - (EI) \quad (3)$$

The observable is the rate of APPNA hydrolysis, which is proportional to E:

$$\text{rate} = E(\text{SA}) \quad (4)$$

where SA is the specific activity in units of ΔOD_{410}/min/pM DP IV active sites at 73.7 μM APPNA. The experimentally variable parameter is I_T. The adjustable parameters to be fit are K_i, E_T (in terms of active sites), and SA. In the case of L-Pro-D-boroPro, the less potent inhibitor, the observed binding appeared to be due to contamination with the L-L diastereomer. This situation was analyzed by including another adjustable parameter, %L-L, in these equations. The actual amount of L-L present therefore was

$$I_T(\text{L-L}) = I_T(\text{L-D})\%\text{L-L}/100 \quad (5)$$

where I_T(L-L) is the true total L-L concentration, I_T(L-D) is the total inhibitor concentration (based upon amino acid analysis), and %L-L is an adjustable parameter describing the % contamination of L-L in the L-D preparation.

Inversion of the Equilibrium Equation To Measure the Rate of Inactivation of L-*Pro*-L-*boroPro.* In the preceding section, an equation was derived describing the observed rate of DP IV catalyzed substrate turnover as a function of the independent variable I_T(L-L) and the parameters K_i, E_T, and SA, which are to be fit to experimental data. Once these parameters have been fit, it is possible to find the inverse relationship to this equation and, with the fitted parameters, to calculate I_T(L-L) from an experimentally measured rate as required for analysis of the DP IV monitored inactivation of Pro-boroPro described above. The following equation is easily derived:

$$I_T(\text{L-L}) = E_T - K_i - \text{rate}/\text{SA} + E_TK_i(\text{SA})/\text{rate} \quad (6)$$

where the parameters are as defined above.

Derivation of an Integrated Rate Equation for the A + B ⇌ C System. Surprisingly, the appropriate form of the integrated rate equation for this system was not found in a number of standard sources. The system

$$E + I \underset{k_{off}}{\overset{k_{on}}{\rightleftharpoons}} (EI) \quad (7)$$

is described by the following set of differential equations

$$d[E]/dt = -k_{on}EI + k_{off}(EI) \quad (8a)$$

$$d[I]/dt = -k_{on}EI + k_{off}(EI) \quad (8b)$$

$$d(EI)/dt = k_{on}EI - k_{off}(EI) \quad (8c)$$

$$I = I_T - (EI) \quad (9)$$

$$k_{off} = k_{on}K_i \quad (11)$$

into the expression for $d(EI)/dt$ and then expansion and rearrangement gives

$$d(EI)/dt = k_{on}(EI)^2 - (k_{on}E_T + k_{on}I_T + k_{on}K_i)(EI) + k_{on}E_TI_T \quad (12)$$

This can be rearranged for integration as

$$dt = \frac{d(EI)}{k_{on}(EI)^2 - (k_{on}E_T + k_{on}I_T + k_{on}K_i)(EI) + k_{on}E_TI_T} \quad (13)$$

The left side of this differential equation is trivial to integrate. The right side is given in standard math tables [*CRC Handbook of Chemistry and Physics*, Vol. 67, p A-26, eq 110, second equation). (Note that we use q for $-q$ and that q in our nomenclature can be shown to always be greater than or equal to 0, a prerequisite for using this equation.)

$$\int dx/X = \frac{1}{\sqrt{q}} \ln\left[\frac{2cx + b - \sqrt{q}}{2cx + b + \sqrt{q}}\right] \quad (14)$$

where $x = (EI)$, $X = a + bx + cx^2$, $a = k_{on}E_TI_T$, $b = -(k_{on}E_T + k_{on}I_T + k_{on}K_i)$, $c = k_{on}$, and $q = b^2 - 4ac$. The appropriate integrated expression is therefore (with an initial condition at $t = 0$ of $x = 0$ (i.e., $(EI) = 0$))

$$t = \frac{1}{\sqrt{q}} \ln\left[\frac{(2cx + b - \sqrt{q})(b + \sqrt{q})}{(2cx + b + \sqrt{q})(b - \sqrt{q})}\right] \quad (15)$$

Rearrangeme..t to solve for x in terms of t gives

$$x = \frac{(1 - e^{t(q)^{1/2}})(b + \sqrt{q})}{2c(e^{t(q)^{1/2}} - ((b + \sqrt{q})/(b - \sqrt{q})))} \quad (16)$$

To check this result, note that at $t = 0$, $x = 0$ as expected. Also note that

$$\text{as } t \to \infty, \quad x \to \frac{(-\infty)(b + \sqrt{q})}{2c(\infty)} \quad (17)$$

$$x = \frac{-b - \sqrt{q}}{2c} \quad (18)$$

which is equivalent to the equilibrium expression derived above (eq 1), also as expected.

Analysis of Enzyme + Substrate Progress Curves. The data were collected at 5-s intervals over the time course of these experiments, up to 1.5 h. Several approaches have been described for the analysis of data of this type. Direct fitting to the integrated Michaelis–Menten equation (Kellershohn & Larent, 1985; Cox & Boeker, 1987) is complicated by the fact that this equation is a mixture of linear and transcendental functions in the dependent variable, and therefore t (time) must be fit as a function of P (product concentration). A more direct approach is to determine the rate (dP/dt) from the data and to fit this directly to the Michaelis–Menten equation (Canela & Franco, 1986). We use this approach here, but have not found it necessary to use a complicated weighting scheme nor to fit the time course data to a polynomial equation to extract derivatives. Instead, the data in terms of [illegible] pairs [illegible] spreadsheet (Lotus Development Corporation, Cambridge, MA). The dt values were calculated by the method of central divided

differences using the formula

$$(dP/dt)_i = (P_{i+1} - P_{i-1})/(t_{i+1} - t_{i-1}) \quad (19)$$

Parameters (K_m and k_{cat}) were then determined by fitting to the Michaelis–Menten equation

$$(dP/dt)_i = k_{cat}S_iE_T/(S_i + K_m) \quad (20)$$

The predicted time course was calculated from the fit parameters by summation using the following equations (Δt = 5s):

$$P_0 = 0 \quad (21)$$

$$S_0 = S_T \quad (22)$$

$$P_i = \sum_{n=1}^{i} (E_T S_{i-1} k_{cat}/(K_m + S_{i-1}))\Delta t \quad (23)$$

$$S_i = S_0 - P_i \quad (24)$$

which can also be performed easily in a Lotus 123 spreadsheet.

Alteratively, the predicted time course can be obtained by numerical integration. The system

$$E + S \underset{k_{-1}}{\overset{k_1}{\rightleftarrows}} (ES) \xrightarrow{k_{cat}} E + P \quad (25)$$

is described by the following set of differential equations:

$$dE/dt = -ESk_1 + (ES)(k_{-1} + k_{cat}) \quad (26a)$$

$$dS/dt = -ESk_1 + (ES)k_{-1} \quad (26b)$$

$$d(ES)/dt = ESk_1 - (ES)(k_{-1} + k_{cat}) \quad (26c)$$

$$dP/dt = (ES)k_{cat} \quad (26d)$$

Given the initial values for the concentrations of the components in this system and values for the rate constants, the GEAR program will provide a simulated time course for comparison with the experimentally determined time course.

Numerical Simulation of the Model Shown in Figure 7A. The model shown in Figure 7A is described by the following set of differential equations:

$$dE/dt = -ESk_1 + (ES)(k_{-1} + k_{cat}) - k_{on}EI + k_{off}(EI) \quad (27a)$$

$$dS/dt = -ESk_1 + (ES)k_{-1} \quad (27b)$$

$$d(ES)/dt = ESk_1 - (ES)(k_{-1} + k_{cat}) \quad (27c)$$

$$dP/dt = (ES)k_{cat} \quad (27d)$$

$$dI/dt = -k_{on}EI + k_{off}(EI) \quad (27e)$$

$$d(EI)/dt = k_{on}EI - k_{off}(EI) \quad (27f)$$

Note that eqs 27 = eqs 8 + eqs 26, i.e., model(Figure 7A) = model($E + I \rightleftarrows EI$) + model($E + S \rightleftarrows ES \rightarrow E + P$). Also note that for the one species common to both models, E, the differential eq 27a is obtained as

$$dE/dt_{\text{model(Figure 7A)}} = dE/dt_{\text{model}(E+I \rightleftarrows EI)} + dE/dt_{\text{model}(E+S \rightleftarrows ES \rightarrow E+P)} \quad (28)$$

Given values for all of the initial concentration and the rate constants describing Figure 7A, it is possible to simulate

RESULTS

Purification of Pro-boroPro Diastereomers. The separation of Pro-boroPro diastereomers by C18 HPLC is shown in Figure

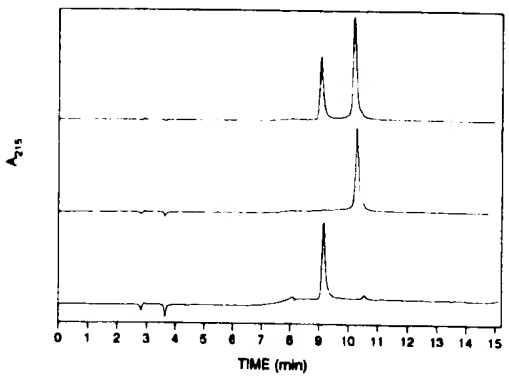

FIGURE 2: C18 HPLC chromatograms showing resolution of Pro-boroPro diastereomers. The upper chromatogram is of the starting mixture, the middle chromatogram is of the purified L-D diastereomer, and the lower chromatogram is of the purified L-L diastereomer. HPLC conditions: solvent A 0.1% trifluoroacetic acid (TFA) in H_2O; solvent B 70% acetonitrile/30% H_2O/0.086% TFA; gradient 0–2 min 0% B, 2–32 min 0–100% B. Only the first 15 min of each chromatogram are shown. The base-line disturbance at 8.15 min is the gradient entering the detector.

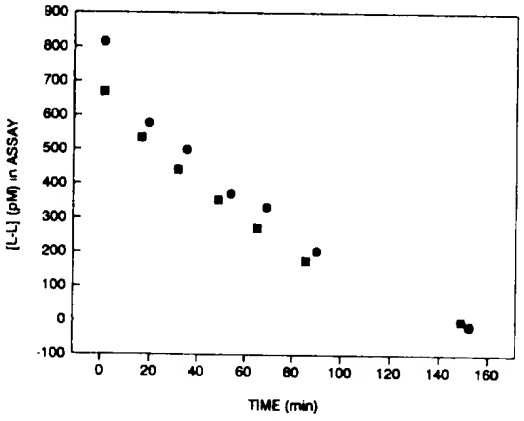

FIGURE 3: DP IV monitored inactivation kinetics of L-L (■) and L-D (●) Pro-boroPro at the very low concentrations (~1 nM of L-L) and pH (7.5) used in the equilibrium and kinetic experiments. The L-L concentration was calculated from the raw data using the inverse of the equilibrium equation derived in the Theory section (eq 6).

2. Attempts to scale up this separation were unsuccessful owing to the decreased resolution with larger column diameters, which could not be overcome by extending the length of the column. For separation on analytical columns, about 0.5 mg of the mixture was loaded for each run. A purity of >98% for the purified products was indicated by analytical HPLC (Figure 2).

Stability of Pro-boroPro Diastereomers. The concentration dependence of the inactivation of Pro-boroPro was examined at very low (~1 nM) and low (~100 nM) concentrations of Pro-boroPro, at pH 7.5, using DP IV inhibition to monitor the residual active inhibitor concentration, and at a relatively high (~250 μM) concentration of the inhibitors using C18 HPLC. The time courses of the degradation kinetics had the same shapes as the curves shown in Figure 3 in all cases, but with somewhat different half-lives. The inactivation reaction [illegible] first-order kinetics with zero-order dominating. The measured half-lives at pH [illegible] for the L-L isomer were 55 min at [illegible] nM, 55 min at [illegible] nM, and 40 min at ~250 μM. The half-life at pH 7.5 for the L-D isomer was somewhat longer: 80 min at ~250 μM as

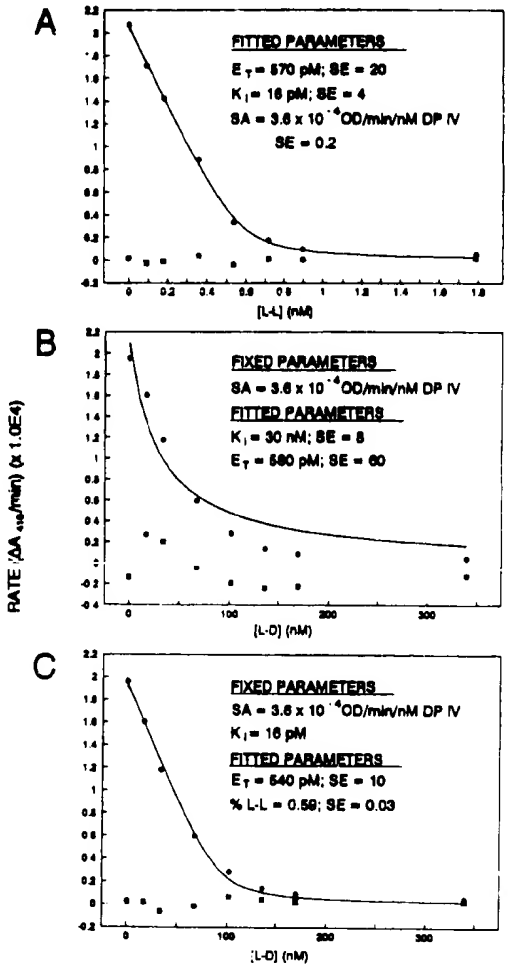

FIGURE 4: Equilibrium titration data and fits obtained for L-L and L-D Pro-boroPro inhibition of DP IV. Each point for the L-L titration is the average of three determinations. Each point for the L-D titration is the average of five determinations. (A) Fit of the L-L titration data to a simple equilibrium model (eq 4). (B) Fit of the L-D titration data to a simple equilibrium model (eq 4). (C) Fit of the L-D titration data to a simple equilibrium model (eq 4) where observed inhibition by L-D is due to contamination by a fractional amount, %L-L, of L-L (eq 5). In this figure, ● is used to represent data points, ■ is used to represent the residual value between the calculated value based upon the fitted parameter and the experimentally observed values, and the lines represent the calculated value of the observable based upon the fitted parameter values.

measured by HPLC. The inactive material can be reactivated by acidification, a process which is relatively slow (85% in 18 h at pH 2.0). The inactive material is the cyclic structure in which the N-terminal nitrogen atom forms a covalent bond with the boron atom of the boronyl group (J. L. Sudmeier, W. G. Gutheil, and W. W. Bachovchin, unpublished results).

Equilibrium Binding of L-L *and* L-D *Pro-boroPro to DP IV.* Under the conditions used for the equilibrium binding assays, >95% of the final equilibrium inhibition was observed in 3 min at the lowest inhibitor concentration used. Free enzyme was assayed after incubating enzyme and inhibitor for 30

Over the [illegible] upward curvature was observed which would indicate inhibitor was being displaced by substrate on this time scale.

The data obtained from the equilibrium binding assays and the statistically fit parameters are shown in Figure 4. These

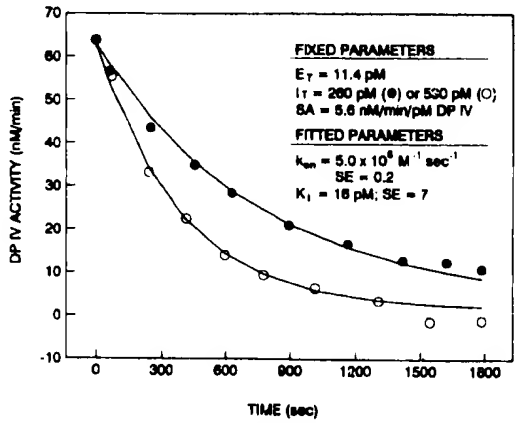

FIGURE 5: Kinetics of L-Pro-L-boroPro binding to DP IV at two inhibitor concentrations. Inhibitor concentrations for the two experiments are shown in the inset. Date were fit to eq 17. Calculated $k_{off} = k_{on}K_i = 78 \times 10^{-6}$ s^{-1}.

experiments yield a K_i for L-Pro-L-boroPro of 16 pM (Figure 4A). This value is much less than the estimated DP IV concentration of 570 pM (SE = 20) (in terms of binding sites) and establishes that the titration was well into the tight binding regime. The L-Pro-D-boroPro binding data fit poorly to the simple equilibrium model (Figure 4B) but very well to a model in which the observed inhibition is assigned to small amounts of contaminating L-Pro-L-boroPro (Figure 4C). This analysis indicated that our preparation of L-Pro-D-boroPro contained 0.59% of the L-L diastereomer and that the inhibition observed with this preparation is due to the contaminating L-L diastereomer. This level of contamination was confirmed by analytical HPLC.

Association and Dissociation Rate Constants for L-Pro-L-*boroPro Binding to DP IV.* To determine values for k_{on} and k_{off}, a more sensitive fluorescent assay was employed to allow the time course of inhibitor binding to DP IV to be monitored under conditions of low DP IV concentration (11.4 pM active sites). A fit of these data to the integrated rate equation derived above (Figure 5) yielded a bimolecular association rate constant, k_{on}, of 5.0×10^6 M^{-1} s^{-1} (SE = 0.2), a K_i of 16 pM (SE = 7) (a value identical with that determined by equilibrium titration), and a unimolecular off rate, k_{off}, calculated from the k_{on} and K_i, of 78×10^{-6} s^{-1}. The calculated off rate indicates that the $t_{1/2}$ for dissociation is 150 min, which is slow relative to the 2 min required for the enzymatic assays employed in these experiments, thereby confirming the original assumption on which this experimental approach was based. This $t_{1/2}$ for dissociation is much longer than the $t_{1/2}$ for the inactivation of free inhibitor and therefore indicates that inhibitor in the enzyme–inhibitor complex is more stable than the free inhibitor.

Kinetics of APPNA Hydrolysis by DP IV. Progress curves for the hydrolysis of APPNA starting at the standard assay concentration of 73.7 μM APPNA are shown in Figure 6A. The fit to the Michaelis–Menten equation using the method described above is very good (Figure 6B), and only a slight difference between the experimental and fit curves is discernible. Product inhibition therefore appears negligible in this case. This analysis yielded a k_{cat} of 90.8 s^{-1} (SE = 0.9)

[illegible] progress curves for enzyme [illegible] inhibitor [illegible] and Numerical Simulation To simulate the hydrolysis of substrate and also the binding and dissociation of inhibitor in the presence of substrate requires the extraction of the

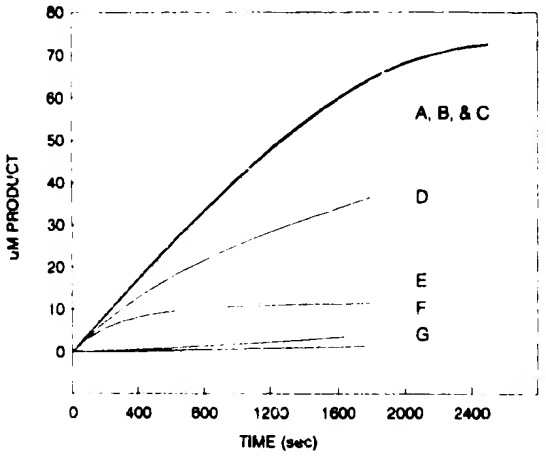

FIGURE 6: Progress curve for the hydrolysis of APPNA in the absence and presence of L-Pro-L-boroPro and fitted and simulated progress curves. (A) Progress curve data for hydrolysis of APPNA by DP IV. The initial concentration of APPNA was 73.7 μM and that of DP IV was 570 pM. (B) Curve resulting from the fit of the progress curve to the Michaelis–Menten equation (eq 20) as described in the text. The fit parameters were K_m = 14.3 μM (SE = 0.4) and k_{cat} = 90.8 s^{-1} (SE = 0.9). (C) Substrate hydrolysis progress curve simulated by numerical integration of eqs 26a–d using $k_1 = 6.34 \times 10^6$ M^{-1} s^{-1}, $k_{-1} = 0$, and $k_{cat} = 90.8$ s^{-1}, as discussed in the text. The curves A–C are essentially indistinguishable. (D) Experimental data from the experiment where DP IV is added to a fresh mixture of APPNA (73.7 μM) and L-Pro-L-boroPro (4.76 nM). (E) Simulation of experiment D by numerical integration of eqs 27a–f with k_1, k_{-1}, and k_{cat} as in C and $k_{on} = 5.0 \times 10^6$ M^{-1} s^{-1} and $k_{off} = 78 \times 10^{-6}$ s^{-1}. (F) Experimental data for the experiment where DP IV is preincubated with L-Pro-L-boroPro (4.76 nM) for 15 min and then APPNA (73.7 μM) is added. (G) Simulation of experiment F by numerical integration.

component rate constants from the K_m:

$$K_m = \frac{k_{-1} + k_{cat}}{k_1} \tag{29}$$

Equation 29 can be rearranged to give

$$k_1 = \frac{k_{-1} + k_{cat}}{K_m} \tag{30}$$

Since k_{-1} must be greater than or equal to 0, k_1 must be greater than or equal to 6.34×10^6 M^{-1} s^{-1} on the basis of the values of K_m and k_{cat} obtained above for DP IV and APPNA. The minimal model for simulating the kinetics of substrate hydrolysis employs values of $k_{-1} = 0$, $k_1 = 6.34 \times 10^6$ M^{-1} s^{-1}, and $k_{cat} = 90.8$ s^{-1}. A simulation of the time course of APPNA hydrolysis by DP IV using these values by numerical integration of eqs 26 gives the result shown in Figure 6, curve C. It is clear that the parameter values obtained using these methods accurately account for the DP IV catalyzed progress curves for APPNA hydrolysis. These values for k_1, k_{-1}, and k_{cat}, together with the determined k_{on} and k_{off} values for L-L Pro-boroPro binding to DP IV, allow the kinetics of a ternary enzyme + substrate + inhibitor experiment, or of substrate being added to preequilibrated enzyme + inhibitor, to be simulated by numerical integration of the differential equations describing Figure 7A (eqs 27). The results from these experiments and simulations are shown in Figure 6, curves [illegible] urately reflect the simplified experiments from which the [illegible] obtained, they do not accurately predict the more comple[illegible] enzyme + substrate + inhibitor experiments. It should be noted that in our simulations the depletion of free enzyme by

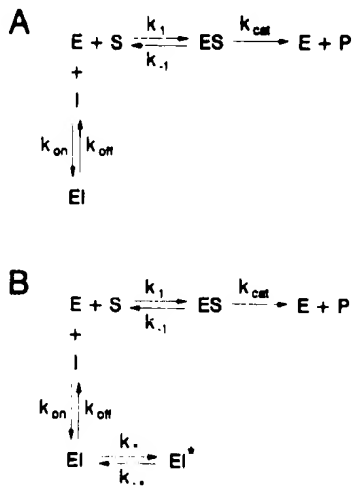

FIGURE 7: Two models for inhibition which have been proposed and used for the analysis of slow-binding inhibitor data: (A) simple model; (B) complex model.

the formation of the *ES* complex is taken into account and that formation of the *ES* complex is rapid and reaches a steady-state concentration in about 10 ms. Increasing the rate at which *ES* reaches the steady state by increasing the value of k_{-1}, and the value of k_1 to satisfy eq 30, has no significant effect on either the simulated substrate hydrolysis progress curve or the simulated enzyme + substrate + inhibitor progress curves.

DISCUSSION

The slow rate at which L-Pro-L-boroPro dissociates from DP IV allows the amount of free enzyme to be sampled during the course of an enzyme plus inhibitor preincubation by the addition of substrate, without the added substrate perturbing the position of the enzyme–inhibitor equilibrium, over the course of a 2-min assay. This simplification in the experimental design allows for a relatively simple mathematical treatment of inhibitor binding to DP IV as an A + B $\rightleftarrows$ C system at equilibrium or approaching equilibrium. Analytical equations for both situations are derived. The integrated rate equation describing the kinetics of such a simple system approaching equilibrium did not appear in standard sources, although we did not search extensively into the older literature. The experimental data were fit directly to these equations, and the reliability of the values for the fit parameters was assessed from the standard errors and from the correlation matrix from the analysis. Other parameters, such as stoichiometry or contamination level, can be included in such an analysis relatively easily, as demonstrated above for the determination of the active site concentration and for the determination that the observed inhibition by our preparation of L-Pro-D-boroPro is due to contaminating L-Pro-L-boroPro.

The experiments were designed to minimize the effect of inhibitor instability on the acquired data, since it was known from previous studies that Pro-boroPro had a half-life of between 30 min and 1 h at pH values of 7.0 and above (Flentke *et al.*, 1991). The equilibrium titrations were therefore [illegible] of nearly high[illegible] centrations of enzyme and inhibitor to ensure that association is complete in 5 min. The equilibrium experiments should have suffered little or perturbation from inhibitor instability. On the other hand, the kinetic experiments had to be conducted at enzyme and

inhibitor concentrations low enough to allow the rate of association to be measured and thus were more susceptible to the effect of inhibitor instability. The effect of inhibitor instability was minimized by restricting the time course to 30 min, during which ~20% of the inhibitor would have decomposed (Figure 3). Thus, even in the kinetic experiments the effects from inhibitor instability should have been small.

The results from the application of this approach to the binding of Pro-boroPro to DP IV demonstrate that L-Pro-L-boroPro is a tight binding inhibitor of DP IV with a K_i of 16 pM. This value is substantially lower than the original estimate of 3 nM, as expected, and more accurately reflects the true affinity of L-Pro-L-boroPro for DP IV. The results also demonstrate that the L-D diastereomer is a much weaker inhibitor than the L-L, if it is an inhibitor at all, as the analysis of the data demonstrates that all of the observed inhibition can be attributed to the presence of ~0.59% of the L-L diastereomer (Figure 4B,C). The bimolecular k_{on} for L-Pro-L-boroPro of 5.0×10^6 M^{-1} s^{-1}, obtained from the kinetic experiments, is close to the values of (5–9) $\times$ 10^6 M^{-1} s^{-1} measured for peptidyl boroArg based inhibitors of thrombin (Kettner *et al.*, 1990). The k_{off} of 78×10^{-6} s^{-1}, calculated from the experimentally determined k_{on} and K_i, indicates that the tight binding of these inhibitors is a consequence of their slow dissociation rates. The slow dissociation of inhibitor ($t_{1/2}$ = 150 min) validates the experimental approach used in this study of preincubating enzyme and inhibitor followed by assaying the enzyme by the addition of substrate.

The tight binding behavior of L-Pro-L-boroPro with DP IV allows it to be used as an active site titrant. The accuracy with which we can measure the concentration of DP IV active sites should be limited primarily by the accuracy with which we can measure the concentration of the stock L-Pro-L-boroPro solution. The concentration of this stock solution was determined from three replicate analyses to be 4.76 mM with a standard error of 0.05 or 1.1%. The results of an active site titration of DP IV with L-Pro-L-boroPro together with the published $\Delta\epsilon$ of 8800 M^{-1} cm^{-1} at 410 nm for substrate hydrolysis (Erlanger *et al.*, 1961), and the progress curve analyses shown in Figure 6B, yield a k_{cat} or turnover number of 90.8 s^{-1}. This is significantly higher than the 54.6 s^{-1} previously reported for this enzyme–substrate pair obtained under slightly different experimental conditions (Heins *et al.*, 1988). The values obtained in this study are less subject to errors owing to protein impurities or denaturation than values based upon protein concentration measurements. Because L-Pro-L-boroPro is a transition-state (or intermediate) analog, only catalytically active enzyme is expected to bind the inhibitor with high affinity. We cannot, however, rule out the possibility that species other than catalytically active DP IV might bind to the inhibitor with sufficient affinity to introduce some error into the use of the stoichiometry for inhibitor binding as a measure of catalytically active DP IV. The estimate of the value for k_{cat} of 90.8 s^{-1} for APPNA hydrolysis under these conditions should therefore be considered as the best current estimate. The true value will in fact be higher if species other than catalytically active DP IV bind this inhibitor with high affinity. The K_m of 14.3 μM obtained here is similar to the previously reported value of 16.6 μM (Heins *et al.*, 1988).

[illegible] Morrison and Walsh (1988)] or a "two-step mechanism" in which a relatively weak enzyme–inhibitor complex is rapidly formed which then undergoes slow conversion to a tighter complex [Figure 7B, mechanism B of Morrison and Walsh (1988)]. The decision of which mechanism is followed should, in principle, be a simple matter of determining which mechanism better accounts for the experimentally observed progress curves. In practice, the discrimination between the one- and two-step mechanisms is not so simple. A major problem is that the integrated forms of the differential equations describing the two-step mechanism (mechanism B) have not been derived owing to their complexity. Consequently, alternative methods have been sought, and the most often used method has been to fit the observed slow-binding progress curves (of enzyme + substrate + inhibitor) to the integrated form of the one-step model (Cha, 1976; Williams *et al.*, 1979). This approach yields values for the initial rate at the beginning of the progress curve, v_0, the final steady-state rate, v_s, and the apparent first-order rate constant for the approach to steady state, k_{obs}. A dependence of v_0 (Williams *et al.*, 1979) or a nonlinear dependence of k_{obs} on inhibitor concentration is taken as evidence for a two-step mechanism (mechanism B). Williams *et al.* (1979) have carried out a more rigorous analysis of the slow-binding inhibition of dihydrofolate reductase by methotrexate by fitting the data to a simulation generated by numerical integration. Such an approach has thus far been reported only once. Williams *et al.* (1979) concluded that the observed inhibition kinetics of DHFR (dihydrofolate reductase) with methotrexate was consistent with a two-step mechanism, but they did not show that the fit to a two-step mechanism was statistically better than that to a one-step mechanism.

The approach we have employed here of preincubating DP IV and L-Pro-L-boroPro in the absence of substrate yields slow-binding curves that both qualitatively and quantitatively resemble slow-binding curves generated in the presence of substrate. A major advantage of this approach is that, owing to the absence of substrate, mathematical analysis of the slow-binding inhibition becomes greatly simplified. The integrated equation for a one-step mechanism in the absence of substrate, however, does not appear to have been derived before and is given in eq 16. A fit of the observed slow-binding kinetics in the absence of substrate to eq 16 is quite good (Figure 5) and yields a K_i value which agrees with that obtained in the equilibrium incubation experiments. This analysis thus indicates that L-L Pro-boroPro binds to DP IV via a one-step mechanism and that the time dependence of the inhibition arises simply as a consequence of low enzyme and inhibitor concentrations. This conclusion is at odds with previous studies of slow-binding inhibition of serine proteases by peptide boronic acids, which have generally favored a two-step mechanism (Kettner & Shenvi, 1984; Shenvi, 1986; Kettner *et al.*, 1988, 1990). Intuitively, it seems that the slow-binding inhibition observed for this class of inhibitors should have a common mechanism and, therefore, that perhaps some of the earlier kinetics supporting two-step binding should be reexamined using the methods reported here. Such studies are in progress.

The parameters obtained for the analysis of the DP IV + L-Pro-L-boroPro data in the absence of substrate accurately account for the data obtained in these experiments (Figures 4 and 5). A problem arises, however, when these parameters are used to simulate the inhibition kinetics observed for the [illegible] of the experimental data in Figure 6D to a numerically integrated rate equation (W. G. Gutheil, unpublished results),

holding the substrate parameters fixed, yields a K_i for the inhibitor of 510 pM, a value substantially higher than that of 16 pM obtained with the simplified system. As the inhibitor concentration is increased, the apparent K_i value decreases, suggesting that the K_i value obtained with the simplified experimental approach represents a limiting value which would eventually be realized at a sufficiently high inhibitor concentration. The apparent dependence of K_i on the inhibitor concentration is inconsistent with either a one- or two-step inhibitor binding mechanism and must therefore reflect some as yet unidentified complication in the enzyme + substrate + inhibitor mixtures which is obviated in the preincubation experiments. The possibility that a component of the substrate solution accelerated the inactivation of the inhibitor has been ruled out (data not shown). Other possibilities include some type of allosteric interaction between the two identical subunits of DP IV or hysteresis.

The experimental approach reported here can be applied to enzyme–inhibitor systems in which the dissociation of the inhibitor is slow relative to the time required to assay the free enzyme. Such an approach has advantages and disadvantages over the traditional method. The main disadvantage is that this approach requires the $t_{1/2}$ for dissociation of the inhibitor to be slow relative to the time necessary for measurement of the enzyme activity. A second disadvantage is that the kinetic measurements require a very sensitive assay capable of measuring the small amounts of enzyme present under kinetic conditions. The major advantage of this approach is that it allows data obtained under both equilibrium and kinetic conditions to be fit directly to analytically derived equations formulated in terms of fundamental physical constants. Another advantage is that it yields kinetic parameters for inhibitor binding under conditions where complications arising from substrate are eliminated. Such an analysis provides a useful starting point for dissecting more complex kinetic systems such as the one described here. We expect that, in the absence of complicating factors, this approach will provide parameters which fully account for the behavior of the enzyme + substrate + inhibitor system. The numerical simulation of complex kinetic systems using experimentally derived rate and equilibrium constants is not commonly used to verify that such constants accurately reflect the data from which they were obtained. The results reported here demonstrate that such an exercise may reveal more complicated interactions between components than originally anticipated.

REFERENCES

Ansorge, S., & Ekkehard, S. (1987) *Acta Histochem. 82*, 41–46.
Bachovchin, W. W., Wong, W. Y. L., Farr-Jones, S., Shenvi, A. B., & Kettner, C. A. (1988) *Biochemistry 27*, 7689–7697.
Bachovchin, W. W., Plaut, A. G., Flentke, G. R., Lynch, M., & Kettner, C. A. (1990) *J. Biol. Chem. 265*, 3738–3743.
Bidlingmeyer, B. A., Cohen, S. A., & Tarvin, T. L. (1984) *J. Chromatogr. 336*, 93–104.
Canela, E. I., & Franco, R. (1986) *Biochem. J. 233*, 599–605.
Cha, S. (1975) *Biochem. Pharmacol. 24*, 2177–2185.
Cha, S. (1976) *Biochem. Pharmacol. 25*, 2695–2702.
Corporale, C., Fontanella, A., Pertrilli, P., Pucci, P., Molinaro, M. F., Picone, D., & Auricchio, S. (1985) *FEBS Lett. 184*, 273–277.
Cox, T. T., & Boeker, E. A. (1987) *Biochem. J 245*, 59–65.
Erlanger, B. F., Kokowsky, N., & Cohen, W. (1961) *Arch. Biochem. Biophys. 95*, 271–278.
Flentke, G. R., Munoz, E., Huber, B. T., Plaut, A. G., Kettner, C. A., & Bachovchin, W. W. (1991) *Proc. Natl. Acad. Sci. U.S.A. 88*, 1556–1559.
Gossrau, R. (1985) *Histochem. J. 17*, 737–771.
Hanski, C., Huhle, T., & Reutter, W. (1985) *Biol. Chem. Hoppe-Seyler 366*, 1169–1176.
Heins, J., Neubert, K., Barth, A., Canizaro, P. C., & Behal, F. J. (1984) *Biochim. Biophys. Acta 785*, 30–35.
Kellershohn, N., & Laurent, M. (1985) *Biochem. J. 231*, 65–74.
Kettner, C. A., & Shenvi, A. B. (1984) *J. Biol. Chem. 259*, 15106–15114.
Kettner, C. A., Bone, R., Agard, D. A., & Bachovchin, W. W. (1988) *Biochemistry 27*, 7682–7688.
Kettner, C. A., Mersinger, L., & Knabb, R. (1990) *J. Biol. Chem. 265*, 18289–18297.
Koehler, K. A., & Lienhard, G. E. (1971) *Biochemistry 10*, 2477–2483.
Kubota, T., Flentke, G. R., Bachovchin, W. W., & Stollar, B. D. (1992) *Clin. Exp. Immunol. 89*, 192–197.
Lindquist, R. N., & Terry, C. (1974) *Arch. Biochem. Biophys. 160*, 135–144.
McKinney, R. J., & Weigert, F. J. (1986) *QCPE No.* QCMPO22
Mentlein, R., Heymann, E., Scholz, W., Feller, A. C., & Flad, H. D. (1984) *Cell. Immunol. 89*, 11–19.
Miyamoto, Y., Ganapathy, V., Barlas, A., Neubert, K., Barth, A., & Leibach, F. H. (1987) *Am. J. Physiol. 252*, F670–F677.
Morrison, J. F., & Walsh, C. T. (1988) *Adv. Enzymol. 61*, 201–300.
Philipp, M., & Maripuri, S. (1981) *FEBS Lett. 133*, 36–38.
Rawn, J. D., & Lienhard, G. E. (1974) *Biochemistry 13*, 3124–3130.
Scholz, W., Mentlein, R., Heymann, E., Feller, A. C., Ulmer, A. J., & Flad, H. D. (1985) *Cell. Immunol. 93*, 199–211.
Schön, E., Mansfeld, H. W., Demuth, H. U., Barth, A., & Ansorge, S. (1985) *Biomed. Biochim. Acta 44*, K9–K15.
Shenvi, A. B. (1986) *Biochemistry 25*, 1286–1291.
Stabler, R. N., & Chesick, J. (1978) *Int. J. Kinet. 10*, 461–469.
Svensson, B., Danielsen, M., Staun, M., Jeppesen, L., Noren, O., & Sjostrom, H. (1978) *Eur. J. Biochem. 90*, 489–498.
Tsilikounas, E., Kettner, C. A., & Bachovchin, W. W. (1992) *Biochemistry 31*, 12839–12846.
Williams, J. W., Morrison, J. F., & Duggleby, R. G. (1979) *Biochemistry 18*, 2567–2573.
Wolf, B., Fischer, G., & Barth, A. (1978) *Acta Biol. Med. Ger. 37*, 409–420.